

ICE-GAN: Identity-aware and Capsule-Enhanced GAN for Micro-Expression Recognition and Synthesis

Jianhui Yu¹, Chaoyi Zhang¹, Yang Song², and Weidong Cai¹

¹ School of Computer Science, University of Sydney, Australia

² School of Computer Science and Engineering, University of New South Wales, Australia

{jianhui.yu, chaoyi.zhang, tom.cai}@sydney.edu.au
yang.song1@unsw.edu.au

Abstract. Micro-expressions can reflect peoples true feelings and motives, which attracts an increasing number of researchers into the studies of automatic facial micro-expression recognition (MER). The detection window of micro-expressions is too short in duration to be perceived by human eye, while their subtle face muscle movements also make MER a challenging task for pattern recognition. To this end, we propose a novel Identity-aware and Capsule-Enhanced Generative Adversarial Network (ICE-GAN¹), which is adversarially completed with the micro-expression synthesis (MES) task, where synthetic faces with controllable micro-expressions can be produced by the generator with distinguishable identity information to improve the MER performance. Meanwhile, the capsule-enhanced discriminator is optimized to simultaneously detect the authenticity and micro-expression class labels. Our ICE-GAN was evaluated on the 2nd Micro-Expression Grand Challenge (MEGC2019) and outperformed the winner by a significant margin (7%). To the best of our knowledge, we are the first work generating identity-preserving faces with different micro-expressions based on micro-expression datasets only.

Keywords: Micro-expression recognition · Micro-expression synthesis · Generative adversarial network · Capsule network

1 Introduction

Micro-expressions display unconscious and restrained feelings that can hardly be perceived by untrained observers [3], making it a challenging pattern recognition task. Due to its potential applications in psychology and security, such as emotional state monitoring and deception detection during interrogation [4], it has attracted an increasing number of researchers into the studies of micro-expression recognition (MER). Although there are many successful works proposed for the conventional expression recognition, the MER domain has not been

¹ <https://github.com/crane-papercode/ICE-GAN>

well-explored, because its detection window is short in duration and there are currently no large-scale datasets available to support extensive MER studies. To this end, we propose the micro-expression synthesis (MES) technique to assist the micro-expression recognition adversarially.

Previous MER methods rely heavily on hand-crafted features such as Local Binary Pattern with three orthogonal planes or six intersection points (LBP-TOP [29] and LBP-SIP [26]). Recently, Convolutional Neural Networks (CNNs) have been applied for MER. STSTNet [12] combines spatial and temporal information embedded in micro-expression video clips to prevent the over-fitting problem. Domain adaptation has also been applied to MER [14], achieving the 1st place in MEGC2019 [20], but it requires an optical flow based preprocessing step. Since these CNN-based approaches are translation invariant and do not encode the position and orientation information of facial object entities, CapsuleNet [19] is adopted for MER [24]. In addition, recently Generative Adversarial Networks (GANs) and their variants [5,15,16,17] have shown their significant generative capabilities in various vision application fields such as facial poses [23], video generation [25], and biomedical image synthesis [28,22]. Taking advantage of CapsuleNet and GAN, CapsuleGAN [9] achieves satisfactory results in simple visual tasks, but has not previously been applied to MER.

The main contributions of our work can be summarized as 3-fold: (1) We design an Identity-aware generator, which produces a synthesis seed as an intermediate latent encoding to preserve the identity information during MES. (2) Our Capsule-Enhanced discriminator aims at distinguishing authenticity and predicting micro-expression labels for input face images, with the position-insensitive issue alleviated by CapsuleNet to improve the MER accuracy. (3) We thereby develop an ICE-GAN framework for Identity-aware MES and Capsule-Enhanced MER, which outperforms the winner of the MEGC2019 Challenge benchmark by a large margin.

2 Method

The optimization process of cGAN [15] can be described as a min-max game where the generator G attempts to synthesize label-controlled fake images to approximate the real data distribution, while the discriminator D is trained adversarially against G to distinguish whether input data is real or synthetic. Mathematically, the learning objective L_{cGAN} can be formulated as:

$$\min_G \max_D V(D, G) = E_{x \sim P_x} [\log(D(x|y))] + E_{z \sim P_z} [1 - D(G(z|y'))]. \quad (1)$$

Our ICE-GAN framework is proposed to extend cGAN with two novel tasks assigned to G and D separately, which could largely improve the overall performance and will be explained in more detail below.

2.1 Model Objective

As its architecture shown in Fig. 1, our ICE-GAN framework consists of an encoder-decoder generator G to synthesize identity-aware expressions, and a

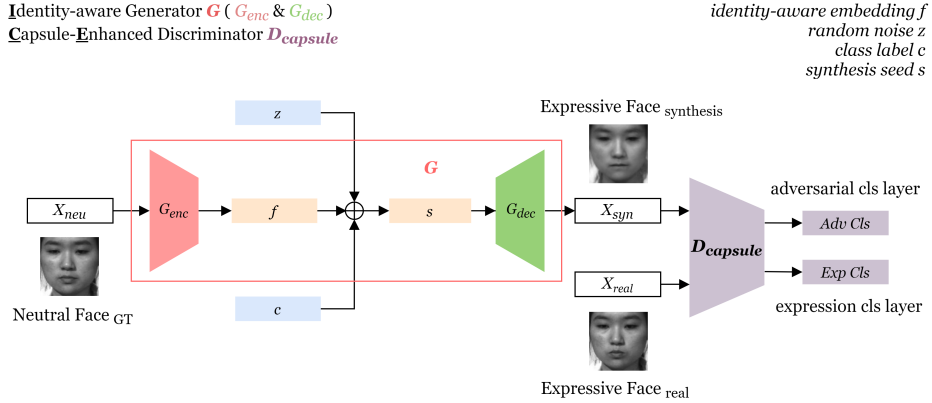


Fig. 1: Architecture of our ICE-GAN framework for MES and MER tasks.

capsule-enhanced discriminator $D_{capsule}$ to discriminate the real/fake labels for the facial images as well as their micro-expression labels simultaneously. The loss function of our proposed ICE-GAN can be formulated as:

$$L_{ICE-GAN}(D, G) = \lambda_{adv} L_{cGAN}(D, G) + \lambda_{MES} L_{IP}(G) + \lambda_{MER} L_{cls}(D), \quad (2)$$

where λ_{adv} , λ_{MES} , and λ_{MER} are the multi-task weighting parameters of our ICE-GAN framework proposed for the tasks of cGAN optimization, identity-aware MES and capsule-enhanced MER, while L_{IP} and L_{cls} are the two task-related constraints specified accordingly.

2.2 Identity-aware Generator for Micro-Expression Synthesis

We designed our identity-aware generator G with an encoder-decoder structure, so that the identity information can be preserved smoothly during the MES procedure. The encoder G_{enc} learns facial attributes from neutral images X_{neu} with a hierarchy of convolutional layers, resulting in an identity-aware embedding $f = G_{enc}(X_{neu})$ in a 512-d latent space. As a controlling term for MES, class label c is aggregated with the encoded f and random noise z to form a synthesis seed $s = [f, z, c]$ in high-dimensional feature space. Then, decoder G_{dec} takes as input the seed s to synthesize identity-aware face images $X_{syn} = G_{dec}(s)$ with controllable micro-expressions. Skip connections are adopted to propagate the multi-scale spatial information between the encoding and decoding processes. The detailed architecture of our identity-aware generator G is shown in Fig. 2.

During the MES progress, we employ a two-term identity-preserving loss L_{IP} for the training of G , to capture and strengthen the identity information encoded in X_{neu} (via G_{enc}) and thus to synthesize distinctive samples X_{syn} (via G_{dec}). One term of L_{IP} is selected as the pixel-wise reconstruction loss L_{pixel} to improve the image quality of X_{syn} . As suggested in [8], we empirically choose L1 penalty over L2 penalty to establish a direct supervision on X_{syn} generated by G . Meanwhile, we also observe the contribution made by maintaining a perceptual

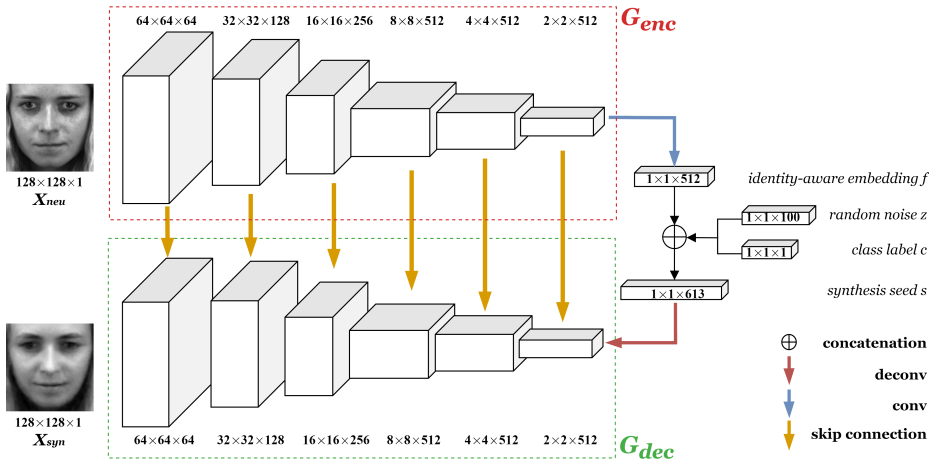


Fig. 2: The encoder-decoder generator G of our ICE-GAN for the MES task.

similarity between X_{neu} and X_{syn} , towards the MES. Hence, a perceptual loss $L_{perceptual}$ [10] is adopted as the second term in our L_{IP} to preserve the facial style information with regards to different subjects. Relying on a cost network $F(\cdot)$ which is usually implemented as a pre-trained CNN, our $L_{perceptual}$ can be easily estimated and minimized over the high-level feature representations associated to X_{neu} and X_{syn} . The overall representation of $L_{IP}(G)$ in Eq. 2 can now be described as:

$$L_{IP}(G) = L_{pixel}(G) + \alpha L_{perceptual}(G). \quad (3)$$

2.3 Capsule-Enhanced Discriminator for Micro-Expression Recognition

Unlike CNNs operating over single scalars, CapsuleNet focuses on the operation over vectors, the lengths of which are used to represent the existence probabilities of each entity in a given image. This design enables the learning of richer visual representations and thus makes CapsuleNet sensitive to the geometric encoding of relative positions and poses of entities, while a conventional CNN fails to capture the position-specific facial information due to its translation-invariance property by nature. CapsuleGAN [9] was the first GAN study utilizing CapsuleNet as its discriminator, which results in a superior performance in modelling simple visual data on the MNIST and CIFAR-10 datasets. Inspired by ACGAN [16], we upgrade the capsule-based discriminator in CapsuleGAN by adding an MER branch that functions as an auxiliary classifier for MER. This enhanced capsule discriminator is dubbed a capsule-enhanced discriminator $D_{capsule}$ in the context of our micro-expression study.

Fig. 3 presents the detailed architecture specifications of $D_{capsule}$. We firstly encode the facial information via *PatchGAN*, such that the learning of the following capsule layers can be converged earlier than being trained from scratch. The

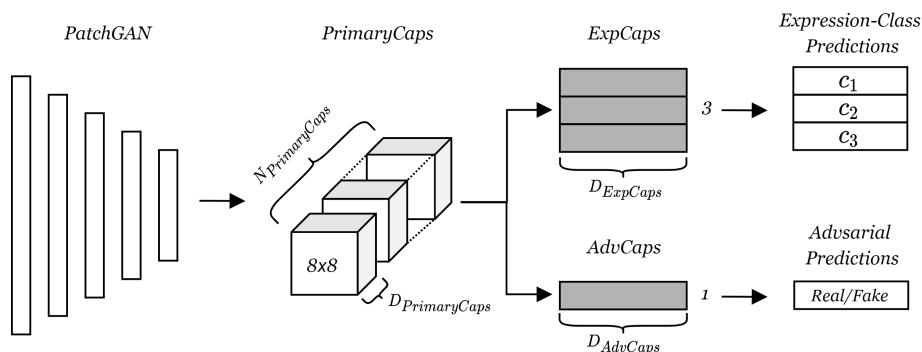


Fig. 3: The capsule-enhanced discriminator $D_{capsule}$ of our ICE-GAN for the MER task.

extracted visual encodings are then fed into *PrimaryCaps*, with the goal of encapsulating the instantiation information at a lower level. Vectors are generated from each individual capsule in *PrimaryCaps*, whose coupling will be further conducted to activate the capsules in the next layer. Following *PrimaryCaps*, two different sub-capsules, namely *AdvCaps* and *ExpCaps*, are constructed to complete two individual sub-tasks for the input images simultaneously: (1) distinguish the real expressive images X_{real} from the synthetic ones X_{syn} , and (2) predict their corresponding micro-expression labels. The *AdvCaps* module is built to detect the authenticity of the input faces, i.e., real/fake, which responds to cGAN optimization. The other sub-capsule module named *ExpCaps* is specifically proposed for the MER task, whose number of capsules equals the number of expression classes. A reconstruction network is desired for a performance gain by regularizing the training of *ExpCaps* [19], which is implemented by three fully-connected layers, with the mean squared error as its reconstruction loss L_{rec} over the reconstructed samples. The learning process is further supervised by a separate margin loss L_{margin} , as suggested in [19], to enlarge the distance between feature encodings belonging to different classes. This L_{margin} can be obtained via:

$$L_{margin}(D) = T_k \max(0, m^+ - \|\mathbf{v}_k\|)^2 + \lambda_k (1 - T_k) \max(0, \|\mathbf{v}_k\| - m^-)^2, \quad (4)$$

where $T_k = 1$ if expression class k exists otherwise 0, while m^+ and m^- are the upper and lower margins and v_k is the vector output of the capsules that being activated to class k . Hence, the overall classification-related loss L_{cls} for our $D_{capsule}$ is summed as:

$$L_{cls}(D) = L_{margin}(D) + \beta L_{rec}(D). \quad (5)$$

2.4 ICE-GAN Framework

With the help of our identity-aware generator, ICE-GAN is capable of approximating the targeted data distribution for MES, with identity-information pre-

served. Meanwhile, relying on the capsule-enhanced discriminator, our model can achieve an excellent performance on facial MER. Based on the descriptions mentioned previously, the final objective of our ICE-GAN is summarized as:

$$L_{ICE-GAN}(G, D) = \lambda_{adv}L_{cGAN}(G, D) + \lambda_{MES}(L_{pixel}(G) + \alpha L_{perceptual}(G)) + \lambda_{MER}(L_{margin}(D) + \beta L_{rec}(D)). \quad (6)$$

3 Experiment

In this section, we firstly compare our ICE-GAN with other state-of-the-art (SOTA) methods proposed for the MER task and our framework outperforms the method ranking 1st on the MEGC2019 benchmark. Extensive studies are then conducted to validate the method design. Additionally, analyses on the image quality of the output generations are reported to verify the capability of our ICE-GAN in the MES task.

3.1 MEGC2019 Challenge Dataset

We evaluate our ICE-GAN on the cross-database MEGC2019 Challenge benchmark, which consists of three publicly available MER datasets (*SMIC* [11], *CASME II* [27] and, *SAMM* [2]). MEGC2019 contains a total of 442 micro-expression video sequences (164, 145 and, 133 clips collected from *SMIC*, *CASME II*, and *SAMM*, respectively), which were captured on 68 subjects (16, 24, and 28 subjects from *SMIC*, *CASME II*, and *SAMM*, respectively). A reduced set of 3-class micro-expressions (positive, negative, and surprise) is shared across these datasets and is thus adopted as the class-label set for the MEGC2019. As requested in [20], we perform Leave-One-Subject-Out (LOSO) cross-validation for subject-independent evaluation under the composite database evaluation (CDE) protocol, i.e., the evaluation experiment is repeated 68 times for all 68 subjects accordingly, until each subject is split alone as the 1-subject testing dataset and with the remaining 67 subjects as the training dataset. Descriptions can be found in [20]. Unweighted F1-score (UF1) and Unweighted Average Recall (UAR) are chosen as the evaluation metrics to make a fair performance comparison under the imbalanced class distribution in MEGC2019, whose calculations can be formulated as follows:

$$UF1 = \frac{1}{C} \sum_i^C \frac{2TP_i}{2TP_i + FP_i + FN_i} \quad \text{and} \quad (7)$$

$$UAR = \frac{1}{C} \sum_i^C \frac{TP_i}{N_i}, \quad (8)$$

where C is the number of classes, while TP_i , FP_i , FN_i , and N_i denote the number of true positives, false positives, false negatives, and total samples belonging to class i , respectively.

3.2 Implementation Details

In this section, we reveal our implementation details of the data preprocessing and the model architecture with training parameters of our ICE-GAN.

Data Preprocessing. Face regions are cropped out by performing facial landmark detection algorithm repeatedly to locate and refine the positions of 68 facial landmarks [6], ending up with a bounding box decided by the refined 68 landmarks with toolkit². Face images with nearly zero expression intensity at the beginning and the end of video clips are referred as *onset* and *offset* frames, respectively, while others with a relatively large expression intensity are denoted as *apex* frames. Annotated positions of *onset*, *apex*, and *offset* frames are available in *CASME II* and *SAMM* but are missing in *SMIC*. Hence, we obtain its *onset* frames (X_{neu}) and *apex* frames (X_{real}) as instructed in [24]. Finally, these cropped face images are resized to 128×128 in grayscale.

ICE-GAN Framework. The multi-task weighting parameters for ICE-GAN are set as follows: $\lambda_{adv} = 0.1$ for cGAN optimization, $\lambda_{MES} = 1$ for identity-aware MES, and $\lambda_{MER} = 1$ for capsule-enhanced MER. Two reweighting ratios α and β are set to 0.1 and 5e-4, respectively. U-Net [18] is employed as the encoder-decoder structure with skip connections in G , with noise dimension $N_z = 100$ and class label dimension $N_c = 1$. VGG-16 [21] pre-trained on ImageNet is chosen as the cost network $F(\cdot)$ for $L_{perceptual}$ estimation. Our $D_{capsule}$ includes a 70×70 *PatchGAN* followed by a *PrimaryCaps* ($N_{PrimaryCaps} = 16$ and $D_{PrimaryCaps} = 8$) and two sub-capsules for classification purposes ($D_{AdvCaps} = 256$ and $D_{ExpCaps} = 32$). m^+ , m^- , and λ_k are set to 0.9, 0.1, and 0.5 for the L_{margin} computation in the adversarial prediction branch of $D_{capsule}$. Adam is selected as the optimizer to train our ICE-GAN framework, with momentums b_1 and b_2 set to 0.5 and 0.999, respectively. The learning rate is initialized as 2e-4 for both G and $D_{capsule}$ and decays with a ratio of 0.9 for every 20 epochs. Batch size is set to 8 and the number of training epochs is 100. The end-to-end training procedure of the ICE-GAN was implemented in Pytorch with 2 Nvidia RTX2080Ti GPUs.

Table 1: MER results on the MEGC2019 benchmark and each individual MER dataset in terms of UF1 and UAR, with LOSO cross-validation.

Method	MEGC2019		SAMM		SMIC		CASME II	
	UF1	UAR	UF1	UAR	UF1	UAR	UF1	UAR
LBP-TOP [29]	0.588	0.578	0.395	0.410	0.200	0.528	0.702	0.742
Quang et al. [24]	0.652	0.650	0.620	0.598	0.582	0.587	0.706	0.701
Zhou et al. [30]	0.732	0.727	0.586	0.566	0.664	0.672	0.862	0.856
STSTNet [12]	0.735	0.760	0.658	0.681	0.680	0.701	0.838	0.868
Liu et al. [14]	0.788	0.782	0.775	0.715	0.746	0.753	0.829	0.820
ICE-GAN	0.845	0.841	0.855	0.823	0.790	0.791	0.876	0.868

² <https://pypi.org/project/face-recognition/>

3.3 Results of Micro-Expression Recognition and Synthesis

LBP-TOP [29] adopts hand-crafted local binary patterns captured from three orthogonal planes and receives a slightly poorer result compared to deep learning approaches. Quang et al. [24] utilizes CapsuleNet structure to achieve acceptable performance, while optical flow based methods [12,14,30] preprocess the raw images to capture the spatiotemporal information from facial movements between *onset* and *apex* images. Liu et al. [14] won MEGC2019 by performing extra domain adaptation from macro- to micro-expression for MER. However, our model and [24] behave differently in that they focus on spatial characteristics of static images only. As shown in Table 1, our ICE-GAN outperforms all existing SOTA approaches on MEGC2019, i.e., our UF1 and UAR scores exceed those of the winner of MEGC2019 by **7.2%** and **7.5%**, respectively. We also achieved the best performance for all per-dataset evaluations.

Rather than generate optical flow images [13], ICE-GAN generates identity-aware faces with three controllable micro-expressions. Apart from all existing micro-expression studies, we analyze the synthetic image quality both qualitatively and quantitatively. The qualitative results of MES evaluation are shown in Fig. 4a, where comparisons between synthetic facial expressions and real samples of four different subjects are demonstrated. The quantitative analysis is developed by calculating the Frchet Inception Distance (FID score [7], also used for our following ablation studies) and FID score of **48.467** is gained by our ICE-GAN under the LOSO cross-validation requested by MEGC2019.

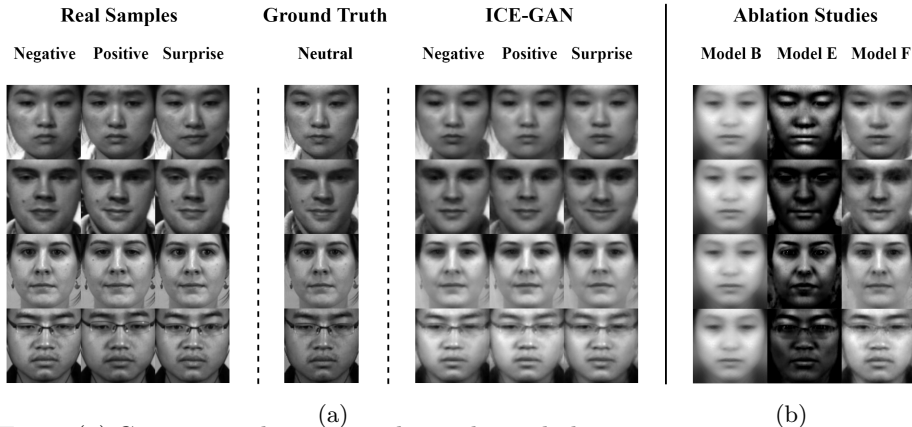


Fig. 4: (a) Comparison between real samples and identity-aware micro-expression faces generated by our ICE-GAN for MES. Neutral images are listed for reference. (b) X_{syn} generated in ablation studies on different generator architectures.

To better illustrate our synthetic micro-expressions with controllable labels, we obtain L2-based difference images between X_{syn} and X_{neu} and focus on action units (AUs) of related muscles. Fig. 5 shows regions of interest for all except the negative faces, which include more than one kind of micro-expression

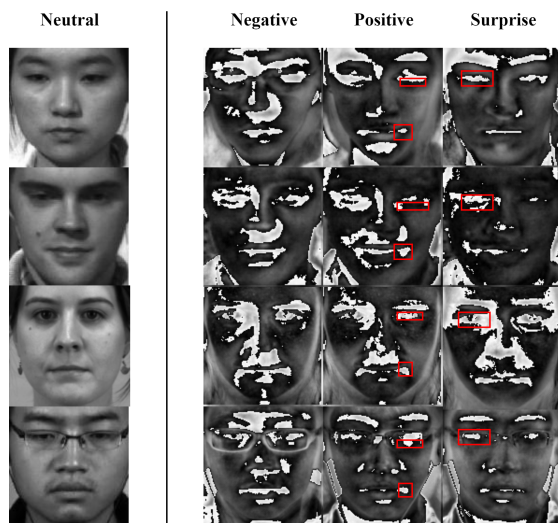


Fig. 5: L2 difference between X_{syn} and X_{neu} . Red boxes indicate the subtle muscle movements associated with the AUs [1].

and therefore makes their patterns challenging to visualize explicitly in detail. Practically, face images can carry compound expressions, so multiple AUs can be activated, but we only care about whether the typical AUs that represent a particular expression exist or not. For positive class, red boxes drawn around the eye area indicate the activation of AU6, and the ones around the lip corner indicate AU12 and AU25. For surprise faces, AU1, AU2, and AU5 are activated, which are all prototypical AUs that are critical for the recognition of positive (i.e., happy) and surprise micro-expressions, according to the Facial Action Coding System [1].

3.4 Ablation Studies

In this section, extensive experiments are performed to validate the component design for our ICE-GAN framework, including G for MES and $D_{capsule}$ for MER. The following ablation studies were conducted on the same MEGC2019 Challenge dataset with a subject-wise splitting ratio set as train : test = 70% : 30%.

Analysis of Generator Design for ICE-GAN. We designed the following ablation studies to verify the effectiveness of various architecture blueprints for our identity-aware G : (1) We first validate the contribution of completing the MES task (the generative adversarial scheme) to assisting our MER task by setting Model A as $D_{capsule}$ (with $ExpCaps$ only) for the micro-expression classification. Specifically, both G and $AdvCaps$ (from $D_{capsule}$), which are associated with the adversarial training framework, are omitted for Model A ; (2) Then, we examine two types of structures that could be utilized to build our

Table 2: Ablation studies on the identity-aware generator design of our ICE-GAN framework. The lower FID is better. Our ICE-GAN development sequence is shown as bold. *SC* is short for skip connections.

Model	$D_{capsule}$		G_I	G_{II}			MER		MES
	<i>ExpCaps</i>	<i>AdvCaps</i>		G_{enc}	G_{dec}	<i>SC</i>	UAR	UF1	FID
A	✓						0.425	0.423	N/A
B	✓	✓	✓				0.651	0.660	196.328
<i>C</i>	✓	✓		✓			0.688	0.682	77.069
<i>D</i>	✓	✓		✓		✓	0.710	0.724	61.758
E	✓	✓			✓		0.705	0.707	75.848
F	✓	✓			✓	✓	0.739	0.745	58.878

identity-aware generator, i.e., G_I and G_{II} , denoting the structure used in DC-GAN and the encoder-decoder architecture, respectively. This setting brings us Model *B* with G_I and Models *C* to *F* with G_{II} ; (3) The difference between *C*/*D* and *E*/*F* is the construction position of our synthesis seed s , decided by whether the identity information is aggregated with z and c prior to G_{enc} (Model *C* and *D*) or prior to G_{dec} (Model *E* and *F*); (4) Meanwhile, we study the influences of multi-scale spatial information propagated through skip connections (Model *D* and *F*) with their corresponding counterparts (Model *C* and *E*).

The essentiality of the generative adversarial framework of our ICE-GAN is demonstrated by comparing Model *A* to others. Model *B* (G_I) achieves a worse result than the other generators (G_{II}), which shows the superiority of the encoder-decoder design in the identity-aware MES. Among the rest, Model *F* gains the best performance on both MER and MES tasks, validating the hypothesis that synthesis seed is better to be constructed with featuremaps containing deeper semantic information, as well as the importance of preserving multi-scale information during the identity-aware MES progress. Moreover, the decrements over FID scores computed by variants of generators shown in Table 2, together with the increased identity information encoded in X_{syn} produced by Models *B*, *E*, and *F* (shown in Fig. 4b), verify our arguments above regarding the effective design of our identity-aware generator for MES progress, both quantitatively and qualitatively. Additionally, the improvements of synthesis quality, which could be viewed in Fig. 4b, demonstrate that finer identity-sensitive facial attributes can be preserved precisely via encoder-decoder architecture ($B \rightarrow E$) and that more high-frequency signals can be passed smoothly through multi-scale skip connections ($E \rightarrow F$), such as the illumination condition.

Overall, since our ICE-GAN framework is developed following the sequence as $A \rightarrow B \rightarrow E \rightarrow F$, the recognition performance (MER) and synthesis quality (MES) gained in each step can be demonstrated numerically in Table 2 and

Table 3: Ablation studies on the capsule-enhanced discriminator design of our ICE-GAN framework.

Method	UAR	UF1	#Params
CNN-based Discriminator	0.347	0.336	6.7 MB
CNN-based Discriminator with comparable size	0.410	0.412	93.0 MB
Capsule-enhanced Discriminator $\mathbf{w/} D_{ExpCaps} = 8$	0.727	0.725	94.4 MB
Capsule-enhanced Discriminator $\mathbf{w/} D_{ExpCaps} = 16$	0.732	0.741	94.6 MB
Capsule-enhanced Discriminator $\mathbf{w/} D_{ExpCaps} = 32$	0.736	0.744	94.9 MB
Capsule-enhanced Discriminator $\mathbf{w/} D_{ExpCaps} = 64$	0.728	0.742	95.8 MB
Capsule-enhanced Discriminator $\mathbf{w/} D_{ExpCaps} = 128$	0.719	0.718	97.4 MB

observed visually in Fig. 4b. Note: our final ICE-GAN and Model F are constructed with the same network architecture and training parameter settings except for evaluation protocols. Specifically, ICE-GAN is trained with LOSO cross-validation requested by the MEGC2019 Challenge, while Model F is optimized with less training data, which is obeyed by all of our ablation studies.

Analysis of Discriminator Design for ICE-GAN. We first exploit the capsule dimension $D_{ExpCaps}$ of $ExpCaps$ within the range of [8, 16, 32, 64, 128] to verify its impacts on the overall MER accuracy. As observed in Table 3, there could be a potential degradation on the framework recognition capability if $D_{ExpCaps}$ is set either too low or too high. The best recognition result is gained by setting $D_{ExpCaps}$ to 32.

We also compare our capsule-enhanced design with its CNN-based counterparts: (1) We replace our two-layer CapsuleNet with a two-layer CNN, while retaining *PatchGAN* architecture in $D_{capsule}$, whose performance is recorded as the 1st row in Table 3. (2) To make a fair comparison of the difference in model size, we then increase the number of neurons in this two-layer CNN and examine the performance of this enlarged CNN-based discriminator (2nd row) on the MER task. As reported in Table 3, our capsule-enhanced discriminator outperforms both of its CNN-based counterparts by a large margin, in terms of UAR and UF1, validating that the capsule-based structure manages to capture the translation-variant facial attributes in a more effective manner.

4 Conclusion

In this work, we propose an ICE-GAN framework for the micro-expression studies, including an Identity-aware generator G of encoder-decoder structure for micro-expression synthesis task, and a Capsule-Enhanced discriminator $D_{capsule}$ for the micro-expression recognition task. Within MES, G extracts identity-sensitive facial attributes that are further aggregated to form a synthesis seed for

the production of controllable expressions, with distinguishable identity information preserved. Furthermore, $D_{capsule}$ enhances MER performance by capturing part-based position-specific face characteristics. Our ICE-GAN is evaluated on the MEGC2019 Challenge and outperforms the winner by a significant margin.

References

1. Cohn, J.F., Ambadar, Z., Ekman, P.: Observer-based measurement of facial expression with the facial action coding system. *The handbook of emotion elicitation and assessment* **1**(3), 203–221 (2007)
2. Davison, A.K., Lansley, C., Costen, N., Tan, K., Yap, M.H.: Sann: A spontaneous micro-facial movement dataset. *IEEE Transactions on Affective Computing (TAC)* **9**(1), 116–129 (2016)
3. Ekman, P., Friesen, W.V.: Nonverbal leakage and clues to deception. *Psychiatry* **32**(1), 88–106 (1969)
4. Frank, M., Herbasz, M., Sinuk, K., Keller, A., Nolan, C.: I see how you feel: Training laypeople and professionals to recognize fleeting emotions. In: *The Annual Meeting of the International Communication Association*. Sheraton New York, New York City (2009)
5. Goodfellow, I., Pouget-Abadie, J., Mirza, M., Xu, B., Warde-Farley, D., Ozair, S., Courville, A., Bengio, Y.: Generative adversarial nets. In: *Advances in neural information processing systems (NeurIPS)*. pp. 2672–2680 (2014)
6. He, Y., Wang, S.J., Li, J., Yap, M.H.: Spotting macro-and micro-expression intervals in long video sequences. *arXiv preprint arXiv:1912.11985* (2019)
7. Heusel, M., Ramsauer, H., Unterthiner, T., Nessler, B., Hochreiter, S.: Gans trained by a two time-scale update rule converge to a local nash equilibrium. In: *Advances in neural information processing systems (NeurIPS)*. pp. 6626–6637 (2017)
8. Isola, P., Zhu, J.Y., Zhou, T., Efros, A.A.: Image-to-image translation with conditional adversarial networks. In: *Proceedings of the IEEE Conference on Computer Vision and Pattern Recognition (CVPR)*. pp. 1125–1134 (2017)
9. Jaiswal, A., AbdAlmageed, W., Wu, Y., Natarajan, P.: Capsulegan: Generative adversarial capsule network. In: *Proceedings of the European Conference on Computer Vision Workshops (ECCVW)*. pp. 526–535 (2018)
10. Johnson, J., Alahi, A., Fei-Fei, L.: Perceptual losses for real-time style transfer and super-resolution. In: *European conference on computer vision (ECCV)*. pp. 694–711. Springer (2016)
11. Li, X., Pfister, T., Huang, X., Zhao, G., Pietikäinen, M.: A spontaneous micro-expression database: Inducement, collection and baseline. In: *2013 10th IEEE International Conference and Workshops on Automatic Face and Gesture Recognition (FG)*. pp. 1–6. IEEE (2013)
12. Liong, S.T., Gan, Y., See, J., Khor, H.Q., Huang, Y.C.: Shallow triple stream three-dimensional cnn (ststnet) for micro-expression recognition. In: *2019 14th IEEE International Conference on Automatic Face & Gesture Recognition (FG)*. pp. 1–5. IEEE (2019)
13. Liong, S.T., Gan, Y., Zheng, D., Li, S.M., Xu, H.X., Zhang, H.Z., Lyu, R.K., Liu, K.H.: Evaluation of the spatio-temporal features and gan for micro-expression recognition system. *Journal of Signal Processing Systems (JSPS)* pp. 1–21 (2020)
14. Liu, Y., Du, H., Zheng, L., Gedeon, T.: A neural micro-expression recognizer. In: *2019 14th IEEE International Conference on Automatic Face & Gesture Recognition (FG)*. pp. 1–4. IEEE (2019)

15. Mirza, M., Osindero, S.: Conditional generative adversarial nets. arXiv preprint arXiv:1411.1784 (2014)
16. Odena, A., Olah, C., Shlens, J.: Conditional image synthesis with auxiliary classifier gans. In: Proceedings of the 34th International Conference on Machine Learning (ICML). pp. 2642–2651. JMLR. org (2017)
17. Radford, A., Metz, L., Chintala, S.: Unsupervised representation learning with deep convolutional generative adversarial networks. International Conference on Learning Representations (ICLR) (2016)
18. Ronneberger, O., Fischer, P., Brox, T.: U-net: Convolutional networks for biomedical image segmentation. In: International Conference on Medical Image Computing and Computer-Assisted Intervention (MICCAI). pp. 234–241. Springer (2015)
19. Sabour, S., Frosst, N., Hinton, G.E.: Dynamic routing between capsules. In: Advances in neural information processing systems (NeurIPS). pp. 3856–3866 (2017)
20. See, J., Yap, M.H., Li, J., Hong, X., Wang, S.J.: Megc 2019—the second facial micro-expressions grand challenge. In: 2019 14th IEEE International Conference on Automatic Face & Gesture Recognition (FG). pp. 1–5. IEEE (2019)
21. Simonyan, K., Zisserman, A.: Very deep convolutional networks for large-scale image recognition. In: International Conference on Learning Representations (ICLR) (2015)
22. Tang, Z., Zhang, D., Song, Y., Wang, H., Liu, D., Zhang, C., Liu, S., Peng, H., Cai, W.: 3d conditional adversarial learning for synthesizing microscopic neuron image using skeleton-to-neuron translation. In: 2020 IEEE 17th International Symposium on Biomedical Imaging (ISBI 2020). pp. 1775–1779. IEEE (2020)
23. Tran, L., Yin, X., Liu, X.: Disentangled representation learning gan for pose-invariant face recognition. In: Proceedings of the IEEE Conference on Computer Vision and Pattern Recognition (CVPR). pp. 1415–1424 (2017)
24. Van Quang, N., Chun, J., Tokuyama, T.: Capsulenet for micro-expression recognition. In: 2019 14th IEEE International Conference on Automatic Face & Gesture Recognition (FG). pp. 1–7. IEEE (2019)
25. Wang, T.C., Liu, M.Y., Zhu, J.Y., Liu, G., Tao, A., Kautz, J., Catanzaro, B.: Video-to-video synthesis. In: Advances in Neural Information Processing Systems (NeurIPS) (2018)
26. Wang, Y., See, J., Phan, R.C.W., Oh, Y.H.: Lbp with six intersection points: Reducing redundant information in lbp-top for micro-expression recognition. In: Asian Conference on Computer Vision (ACCV). pp. 525–537. Springer (2014)
27. Yan, W.J., Li, X., Wang, S.J., Zhao, G., Liu, Y.J., Chen, Y.H., Fu, X.: Casme ii: An improved spontaneous micro-expression database and the baseline evaluation. *PLoS one* **9**(1) (2014)
28. Zhang, C., Song, Y., Liu, S., Lill, S., Wang, C., Tang, Z., You, Y., Gao, Y., Klishtorner, A., Barnett, M., et al.: Ms-gan: Gan-based semantic segmentation of multiple sclerosis lesions in brain magnetic resonance imaging. In: 2018 Digital Image Computing: Techniques and Applications (DICTA). pp. 1–8. IEEE (2018)
29. Zhao, G., Pietikainen, M.: Dynamic texture recognition using local binary patterns with an application to facial expressions. *IEEE Transactions on Pattern Analysis and Machine Intelligence (TPAMI)* **29**(6), 915–928 (2007)
30. Zhou, L., Mao, Q., Xue, L.: Dual-inception network for cross-database micro-expression recognition. In: 2019 14th IEEE International Conference on Automatic Face & Gesture Recognition (FG). pp. 1–5. IEEE (2019)